Computational Materials Science 78 (2013) 74–82

Contents lists available at SciVerse ScienceDirect

Computational Materials Science

journal homepage: www.elsevier.com/locate/commatsci

Modeling and simulation of the TiC reaction layer growth during active brazing of diamond using DICTRA

W.J. Zhu [a,b], J. Wang [a,c], L.B. Liu [b,d], H.S. Liu [b,d], Z.P. Jin [b,d], C. Leinenbach [a,*]

[a] Empa-Swiss Federal Laboratories for Materials Science and Technology, Laboratory for Joining Technologies and Corrosion, Überlandstrasse 129, CH-8600 Dübendorf, Switzerland
[b] School of Materials Science and Engineering, Central South University, Changsha, Hunan 410083, PR China
[c] School of Materials Science and Engineering, Guilin University of Electronic Technology, Guilin, Guangxi 541004, PR China
[d] Education Ministry Key Laboratory of Non-ferrous Materials Science and Engineering, Central South University, Changsha, Hunan 410083, PR China

ARTICLE INFO

Article history:
Received 16 April 2013
Received in revised form 3 May 2013
Accepted 14 May 2013
Available online 15 June 2013

Keywords:
Cu–Sn–Ti alloy
TiC
Diffusion
Atomic mobility
Kinetic simulations
CALPHAD
DICTRA

ABSTRACT

The growth kinetics of the TiC reaction layer during active brazing of diamond with Cu–Sn–Ti and Ag–Cu–Ti based filler alloy has been investigated by kinetic simulations and comparing with available experimental data. First, to obtain a reliable mobility database, the atomic mobilities of C and Ti in fcc (face-centered cubic) TiC are assessed using software DICTRA based on available diffusion data from literatures. Then, to carry out simulations for GB (Grain Boundary) diffusion in TiC, the bulk activation energy multiplier is determined by evaluating the available GB diffusion data. With the obtained mobility data, the TiC growth for Cu–Sn–Ti–Zr filler as a function of brazing temperature and time is simulated using various possible GB diffusion parameters. Afterwards, the determined GB diffusion parameters are validated by simulating the TiC growth for various Cu–Sn–Ti or Ag–Cu–Ti brazing alloys and comparing the simulated results with experimental data. Based on the optimized GB diffusion parameters, the influence of brazing temperature, filler alloy composition, and braze layer thickness on growth kinetics of TiC are simulated and discussed. Finally, the experimentally observed segregation of Cu at the interface between diamond and TiC layer during brazing of diamond using Cu–Sn–Ti or Ag–Cu–Ti filler is analyzed by diffusion simulations.

1. Introduction

Joining of advanced ceramics or super hard materials such as diamond or cubic boron nitride (cBN) to metallic substrates like Cu, Fe and Ni-based alloys has become an important manufacturing step for many industrial applications because it combines the advantageous mechanical and chemical properties of various materials in the same component [1–5]. In particular diamond is a preferred abrasive component in high performance grinding tools for drilling, milling, grinding, and sawing of hard materials like ceramics, hardened steel, hard metals, glass, concrete and granite because it combines high hardness, high strength, high wear resistivity and chemical inertness.

Active brazing with Ag-, Cu-, Ni- or Cu–Sn-based braze alloys is a widely used technique for joining diamond or ceramics to metals. It is well known that liquid Ag, Au, Cu or Sn do not wet diamond [6]. Therefore, brazing of diamond can be only made possible by addition of active elements such as Ti, V or Cr, which form a wettable interfacial carbide reaction layer [7–10]. If Ti is added, it has been reported that a TiC layer forms epitaxially on the diamond which is wetted by the liquid braze alloy [11–14]. For Cu–Sn–Ti alloys, the layer consists of an inner layer of nano-sized, C-rich cuboidal TiC crystals and a second layer of Ti-rich columnar TiC crystals. While the inner layer does not vary with the brazing parameters, the thickness of the second layer is a function of the brazing time and temperature [14]. Li et al. [11,12] reported that no other transitional phase occurs between diamond (100) and (110) planes, respectively, and the TiC layer when diamond grits reacted with a Cu–Sn–Ti alloy. However, Khalid et al. [13] observed a thin Cu-rich layer formed at the diamond surface at the interface between diamond grit and Cu–Sn–Ti–Zr brazing alloy. Klotz et al. [14] observed the formation of a thin Cu-rich layer directly between diamond (111) planes and TiC during brazing with different Cu–Sn–Ti alloys. The growth kinetics of the TiC layer or the Cu-rich layer can play an important role for the formation of residual stresses and defects in the diamond and the TiC due to the mismatched thermal expansion coefficients and lattice parameters [15]. The caused stresses and defects can be highly detrimental and may induce weakening and failure of the braze joint [16]. Therefore, it is important to simulate and control the growth behavior of the TiC reaction layer during brazing of diamond.

The aim of the present work is to simulate the growth kinetics of the TiC reaction layer formed at the diamond-filler interface

* Corresponding author. Tel.: +41 58 765 4518; fax: +41 58 765 4039.
E-mail address: christian.leinenbach@empa.ch (C. Leinenbach).

0927-0256/$ - see front matter © 2013 Elsevier B.V. All rights reserved.
http://dx.doi.org/10.1016/j.commatsci.2013.05.025

during active brazing of diamond with Cu–Sn–Ti or Ag–Cu–Ti based brazing alloys. To achieve this, the associated mobility database is necessary. Hence, as a first step, the atomic mobilities of C and Ti in fcc TiC need to be assessed using the Andersson–Ågren method [17,18] and the DICTRA (DIffusion Controlled TRAnsformation) software package [17–19] based on the available experimental diffusion data. Then, various parameters, e.g. activation energy multiplier, grain size, and grain boundary thickness regarding grain boundary diffusion in TiC, need to be determined to enable more reasonable simulations. After that, the effect of brazing temperature, filler alloy composition and braze layer thickness on the growth of TiC are investigated. Finally, the segregation of Cu at the diamond-filler alloy interface which was observed in many experiments is analyzed and interpreted by diffusion simulation.

2. Modeling and simulation method

2.1. Theory

In this part, the fundamental theory and/or methods concerning the simulation of the growth of TiC formed during brazing of diamond are introduced. The DICTRA [17–19] software is used as a tool for modeling atomic mobilities in phases of interest and simulating kinetics of diffusion-controlled transformation. A local equilibrium assumption is accepted in the software system so that no difference exist in chemical potential across phase interface, and concentrations of components at the phase interface can be evaluated from the relevant phase diagrams. The assumption has proven to be accurate enough to simulate diffusion-controlled transformations [20–22], even though it may deviate owing to some possible effects from curved interfaces, finite mobility of interface, solute drag, and elastic stresses.

Considering the investigations of brazing of diamond with various filler alloys [11–14], a cuboidal TiC layer with a thickness of approximately 50 nm, independent of the filler alloy composition and brazing parameters, forms first on the diamond. On top of this cuboidal TiC layer, a columnar TiC layer grows as a function of filler alloy composition as well as of the brazing temperature and time. The growth of the columnar TiC layer is only controlled by movement of the interface between the columnar TiC layer and the filler alloy. In order to analyze and simulate the growth of the TiC layer, a model as shown in Fig. 1 is established by simplifying the growth mode to a one-dimensional geometry. In the model, the simulation domain is composed of two distinct regions. The region on the left-hand side is defined as an fcc TiC reaction layer, while the right-hand side is defined as a liquid filler phase of a Cu–Sn–Ti or Ag–Cu–Ti based alloy. The two regions are separated by a planar interface. Based on the local equilibrium assumption, the interface migration is controlled by the rate of atomic diffusion across the interface and also determined by the mass balance, which yields a flux balance condition at the migrating interface [19,23]. The flux balance equation is formulated as follows:

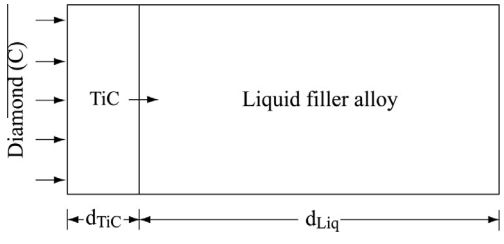

Fig. 1. Model used in the DICTRA simulation for the growth of the TiC reaction layer.

$$v^{liq}C_k^{liq} - v^{TiC}C_k^{TiC} = J_k^{liq} - J_k^{TiC} \quad (k = 1, 2, \ldots, n) \tag{1}$$

where v^{liq} and v^{TiC} are the rate of the interface migration, C_k^{TiC} and C_k^{liq} are the concentrations of components k in TiC and liquid filler close to the phase interface, and J_k^{TiC} and J_k^{liq} are the diffusional fluxes in TiC and liquid filler, respectively.

In a multi-component system, diffusional flux J_k will depend on the concentration gradients of all independent elements in the system. This condition is expressed by the Fick–Onsager law:

$$J_k = -\sum_{j=1}^{n-1} D_{kj}^n \nabla C_j \tag{2}$$

where ∇C_j is concentration gradient of component j, D_{kj}^n is a $(n-1)\times(n-1)$ chemical diffusivity matrix for a solution phase. The summation is performed over $(n-1)$ independent concentration as the dependent n may be selected as the dependent component. Because mobility of a component is the basic kinetic parameter relating diffusion flux, the chemical diffusivity D_{kj}^n is usually related to the mobility by the following expression [17,18]:

$$D_{kj}^n = \sum_i (\delta_{ik} - x_k) x_i M_i \left(\frac{\partial \mu_i}{\partial x_j} - \frac{\partial \mu_i}{\partial x_n}\right) \quad \text{(when } j \text{ is substitutional)} \tag{3a}$$

$$D_{kj}^n = \sum_i (\delta_{ik} - x_k) x_i M_i \left(\frac{\partial \mu_i}{\partial x_j}\right) \quad \text{(when } j \text{ is interstitial)} \tag{3b}$$

where δ_{ik} is the Kronecker delta ($\delta_{ik} = 1$ if $i = k$, otherwise $\delta_{ik} = 0$), x_i the mole fraction, μ_i the chemical potential of component i, and $\partial\mu_i/\partial x_j$ is related to the thermodynamic factor, which can be obtained by thermodynamic calculation with the associated thermodynamic database. M_i is the composition dependent atomic mobility of i for bulk diffusion.

Based on the absolute reaction rate theory, the mobility parameter M_i can be divided into a frequency factor M_i^0 and an activation energy Q_i. In general, both M_i^0 and Q_i are dependent on temperature, composition, and pressure. According to the suggestion by Jönsson [24,25], the M_i can be expressed as:

$$M_i = \exp\left(\frac{RT\ln M_i^0}{RT}\right)\exp\left(\frac{-Q_i}{RT}\right)\frac{1}{RT}\,{}^{mg}\Omega \tag{4}$$

where R is the gas constant, T the temperature, and ${}^{mg}\Omega$ is a factor taking into account a ferromagnetic contribution to diffusion. For non-bcc phases, the influence of ferromagnetism on diffusion is negligible, i.e., ${}^{mg}\Omega = 1$ [26]. As a consequence, it is sufficient to combine $RT\ln M_i^0$ and Q_i into one parameter ΔG_i^{ϕ} by $\Delta G_i^{\phi} = RT\ln M_i^0 - Q_i$. Eq. (4) can be thus simplified as:

$$M_i = \exp\left(\frac{\Delta G_i^{\phi}}{RT}\right)\frac{1}{RT} \tag{5}$$

Similar to the phenomenological CALPHAD method, Andersson and Ågren [18] suggested that the parameter ΔG_i^{ϕ} can be assumed to be a composition dependent function, which can be expressed by a Redlich–Kister polynomial [27]. For the fcc TiC, ΔG_i^{ϕ} is given as follows:

$$\Delta G_i^{\phi} = y_{Ti}^{I} y_C^{II} \Delta G_i^{Ti:C} + y_{Ti}^{I} y_{Va}^{II} \Delta G_i^{Ti:Va} + y_{Ti}^{I} y_C^{II} y_{Va}^{II} \sum_{j=0}^{n} \Delta^{(j)} G_i^{Ti:C,Va} (y_C^{II} - y_{Va}^{II})^j \tag{6}$$

where y_{Ti}^{I}, y_C^{II} and y_{Va}^{II} are site fraction of Ti, C or Va in sublattice I or II, and $\Delta G_i^{Ti:C}$ and $\Delta G_i^{Ti:Va}$ are values of the $\Delta G_i^{\varphi}(i = C, Ti)$ respectively for stoichiometric fcc $(Ti)_{0.5}$:$(C)_{0.5}$ and hypothetical pure fcc(Ti), and thus represent the endpoint values in the composition space, while $\Delta^{(j)} G_i^{Ti:C,Va}$ is a binary interaction term for i diffusion between C and Va.

As for the growth of TiC during active brazing of diamond, it is observed that the size of the TiC grain or layer varies on the nanoscale [11–14]. Grain boundaries in the TiC layer, being highly disordered atomic structures compared to the adjoining crystal lattices, act as fast diffusion paths for the host as well as for impurity atoms. Thus, diffusion of atoms in the grain boundaries of the TiC layer should be considered for simulating the growth of the TiC layer. Fortunately, grain boundary diffusion has been implemented in the DICTRA software package with an assumption that it contributes to total diffusion by using the same frequency factor and modified bulk activation energy. The grain boundaries will contribute to the total amount of diffusion according to their weighted fractions. The atomic mobility M_i^{gb} of i in the grain boundary is expressed as follows:

$$M_i^{gb} = M_i^0 \exp\left(\frac{-F_{redGB} \cdot Q_i}{RT}\right)\frac{1}{RT} \tag{7}$$

where R is the gas constant, T the Kelvin temperature, M_i^0 and Q_i are respectively the frequency factor and activation energy for bulk diffusion of i, and F_{redGB} is the bulk diffusion activation energy multiplier. As a result, the weighted calculated value for the overall mobility M_i^* is then evaluated from:

$$M_i^* = \left(\frac{\delta}{d}\right) \cdot M_i^{gb} + \left(1 - \frac{\delta}{d}\right) \cdot M_i \tag{8}$$

where δ is the grain boundary thickness, d the grain size, M_i the atomic mobility of i in the bulk, and δ/d is the fraction of grain boundaries in the bulk.

2.2. Simulation conditions

In order to simulate the growth of the TiC layer, relevant databases are required. The thermodynamic databases are available and taken from the literature [28–36], while the diffusion databases need to be developed. According to the criteria set by Kirkarldy and Young [37], diffusion coefficients of all elements in a liquid phase can be approximated by a constant value of 1×10^{-9} m^2/s, which is adopted in this work. With regard to the experimental observations in [13,14], TiC is almost composed of only C and Ti, and solid solubilities of Ag, Cu and Sn in TiC are negligible. Additionally, no systematic data for diffusion coefficients of Ag, Cu, Sn and Zr in TiC are available in literature. Consequently, atomic mobilities of only C and Ti in TiC are considered in simulating the growth of the TiC layer. The atomic mobilities are to be assessed and discussed in the later chapters.

To enable successful running of the simulations in the DICTRA environment, various setting conditions, e.g., distribution of grid points used for numerical computation in the regions of TiC and filler alloy, boundary constraint conditions, brazing temperatures and holding time to be simulated, initial thicknesses and compositional profiles of the TiC layer and the filler alloy layer, are required.

Owing to the sharp compositional gradient at interface between the TiC and the filler, a higher density of grid points has to be used on both sides of the interface. Because diamond has almost no solubility for other elements, and since the growth of the TiC layer is mainly controlled by diffusion of C from the diamond through the TiC layer (cf. Section 3), the diamond can be thus regarded as a carburization source. As a consequence, mixed boundary conditions involving constant activity for C and zero flux for other elements are used on the left side of the computational domain, while zero flux condition for all elements is used on the right side. The simulated temperatures are directly referred to typical process temperatures in brazing of diamond, which are usually in the range from 800 °C to 980 °C, depending on the filler alloy. The simulated time in the present work is usually explored up to 1 h, which is longer than usual brazing time of 10–30 min. The initial thickness d_{TiC} of the TiC reaction layer is determined to be 50 nm, which is evaluated from the results of TEM (Transmission Electron Microscope) and SEM (Scanning Electron Microscope) investigations [13,14]. The initial thickness d_{Liq} of the filler layer, i.e. the brazing layer thickness, usually varies in the range from 1 to 100 μm with a typical value of 50 μm for brazing of diamond. The influences of the braze layer thicknesses of 1, 10, 50 and 100 μm were thus investigated in the present work. The initial compositions of the filler layer are directly taken from the compositions of brazing alloys used. As for the initial composition of the TiC layer, i.e. the composition of the cuboidal TiC layer initially formed onto diamond, it is measured to be 60 at.% C [13], which should be unreasonable according to the Ti–C phase diagram [28] and solubilities of other elements in TiC [14].

In order to obtain reasonable values for the initial compositions of the TiC layer, Lee et al.'s scheme [38] is herein adopted that the driving force for nucleation of an interfacial reaction product can be evaluated by calculating metastable equilibria among adjacent phases, and the composition of a critical nucleus of the product can be assessed by searching the maximum driving force of the nucleation. Considering the formation of the TiC layer in the initial stage of the reaction between diamond and liquid filler, the composition of a critical nucleus of TiC might be a good approximation of initial composition of the TiC layer. The driving force for the nucleation of TiC ΔG_m^{nucl} can be obtained by the expression:

$$\Delta G_m^{nucl} = \sum_{j=C,Ti,\ldots} x_j^{TiC}\mu_j^{liq}(x_C^{liq/diamond}, x_{Ti}^{liq/diamond}, \ldots, x_j^{liq/diamond}) - G_m^{TiC}(x_C^{TiC}, x_{Ti}^{TiC}) \tag{9}$$

where x_j^{TiC} is the mole fraction of component j in the TiC particle nucleus, $x_j^{liq/diamond}$ is the mole fraction of j in liquid filler close to the phase interface between liquid and diamond, μ_j^{liq} is the chemical potential of j in the liquid filler, G_m^{TiC} is the molar Gibbs energy of the TiC particle. From Eq. (9), the compositions of the critical nucleus of TiC x_j^{TiC}, as the approximation of the initial compositions of the TiC layer, can be assessed by thermodynamic calculations to be in C-rich range, which is in agreement with the measurements [13,14].

3. Assessment of atomic mobilities in bulk fcc TiC

3.1. Literature information

Regarding the self-diffusion of C in bulk TiC, many investigations have been previously published. Eremeev and Panov [39] studied diffusion of C in $TiC_{0.47}$ and obtained a temperature dependent expression for the diffusion coefficients in the temperature range of 1780–2110 °C. Sarian [40] measured self-diffusion coefficients of C in $TiC_{0.970}$ and $TiC_{0.887}$ in the temperature range from 1450 °C to 2280 °C. The effect of composition on the self-diffusion coefficients was analyzed by using Arrhenius equations and found that the diffusional pre-exponential factor D_0 and activation energies Q increased with decreasing C contents, indicating that C diffuses by an octahedral vacancy mechanism. In addition, Sarian [41] investigated self-diffusion of C in $TiC_{0.67}$ in the temperature range from 1745 °C to 2720 °C and represented two different Arrhenius expressions respectively for the temperature ranges below and above 2080 °C. Based on these studies [39–41], a composition-dependent critical temperature exists and forms the boundary between two modes of C diffusion. Each mode has a set of temperature-independent, composition-dependent Arrhenius coefficients D_0 and Q. Below the critical temperature, D_0 is proportional to

the apparent C deficiency, while Q increases with increasing numbers of C vacancies.

Only a few investigations regarding self-diffusion of Ti in bulk TiC are reported in the literature. Sarian [42] studied self-diffusion of Ti in TiC_x $(0.67 \leqslant x \leqslant 0.97)$ in the temperature range 1920−2215 °C. The diffusion coefficients are found to be composition independent and can be described by a unified expression. It was also found that Ti diffuses by a factor of approximately 10^4 slower than C in the considered temperature range.

A number of investigations [43–47] on the chemical diffusion in a reaction-grown TiC layer have been reported, but only values of an average diffusion coefficient were presented. Kohlstedt et al. [48] measured the inter-diffusion coefficient $\tilde{D}$ in TiC_{1-y} as a function of y, and reported an increasing value of $\tilde{D}$ from $TiC_{0.86}$ to $TiC_{0.97}$. This increasing value of $\tilde{D}$ with an increasing C concentration seems to be unreasonable due to lower diffusivity caused by corresponding less amounts of vacancies in TiC. van Loo et al. [49] measured the chemical diffusion coefficient of C in TiC_{1-y} as a function of the stoichiometry and temperature in the range between 1200 and 1750 °C. The diffusion coefficient was found to increase with decreasing C concentration, which is acceptable. The chemical diffusion coefficient of C in TiC_{1-y} was also determined by van Loo and Bastin [50] in the temperature range of 1000–1600 °C using the diffusion couple technique. The diffusion coefficient was found to increase with decreasing C concentration. The activation energy for the chemical diffusion process is virtually independent of composition. In addition, Albertsen and Schaller [51] measured the chemical diffusion coefficient of C in TiC over the entire phase field between 1179 and 2413 K using suitably designed diffusion couples. The diffusion coefficients increased with decreasing C content, which is in agreement with the results from van Loo et al. [49,50].

3.2. Comparison between calculated results and literature data

In order to extract the mobility parameters, reasonable thermodynamic descriptions are required for calculating the thermodynamic factor. The thermodynamic database of the C–Ti binary system from Frisk [28] has been used in the present work, which can reproduce the phase diagram and most of thermodynamic data. The self-diffusion coefficient of Ti in the hypothetical fcc Ti cannot be determined by experimental methods because of its unstable structure at 298.15 K and 1 bar. The self-diffusion coefficient of Ti was assessed by Matan et al. [52] and Campbell et al. [53] through an empirical analysis. The mobility parameter of Ti determined by Matan et al. [52] was thus used in the present work. According to Eq. (6), the impurity diffusion coefficient of C in hypothetical fcc Ti is required but cannot be measured experimentally. Because both hcp and fcc crystal structure of Ti are close-packed and would present a similar kinetic behavior, the impurity diffusion coefficients of C in hypothetical fcc Ti is taken from the data measured for hcp Ti [54]. Since the diffusion for the hcp is non-isotropic, an average value considering the mobility values parallel and perpendicular to the basal plane was used. Any other mobility parameters of C and Ti in fcc TiC were subject to the optimization in the present work.

The optimization for obtaining the atomic mobilities was performed using the PARROT module of the DICTRA software package [17–19]. The module works by minimizing the square sum of the differences between experimental data and calculated values. In the present optimization, the experimental data of tracer self-diffusion coefficients and chemical diffusion coefficients reported by Eremeev and Panov [39], Sarian et al. [40–42], Kohlstedt et al. [48], van Loo et al. [49,50], Albertsen and Schaller [51] are employed to assess the mobility parameters of C and Ti for the fcc TiC alloys.

Fig. 2 is the calculated phase diagram of the Ti–C binary system and Fig. 3 shows the calculated thermodynamic factor of the fcc TiC alloys at different temperatures using the thermodynamic parameters [28].

Fig. 4a presents the calculated temperature dependence of C self-diffusion coefficients in fcc TiC (with different C contents) with the experimental data [39–41]. The calculated results are in good agreement with the experimental data reported in [40,41], but show a deviation from the experimental data of Eremeev and Panov [39]. The impurity effect and the large inaccuracy of the temperature measurement in the work [39] could be the reason for the deviation. A comparison between the calculated self-diffusion coefficients of Ti in fcc TiC and the experimental data [42] is given in Fig. 4b. The calculated results agree well with the experimental data if the usual error ranges of the diffusion coefficients are considered. The calculated temperature dependence of the chemical inter-diffusion coefficients in fcc TiC alloys is compared with the experimental data measured by Kohlstedt et al. [48], van Loo et al. [49,50], Albertsen and Schaller [51] as shown in Fig. 4c. The calculated inter-diffusion coefficients as a function of temperature are in good agreement with the experimental data. Fig. 4d shows the calculated concentration dependence of inter-diffusion coefficients in fcc TiC alloys. The calculations reproduce satisfactorily the experimental data [49–51].

In general, the calculation results are in reasonably good agreement with the literature data. The mobility parameters obtained in the present work are finally summarized in Table 1.

4. Simulation results and discussion

4.1. Influence of grain boundary thickness and grain size of TiC

The bulk diffusion activation energy multiplier, as the important parameter for simulating grain boundary (GB) diffusion, is firstly determined by fitting the available bulk and GB diffusion data [40,55–58] of other metallic carbides which represent a similar kinetic behavior as shown in Fig. 5. An average multiplier of 0.81637 is determined, which will be applied in the later simulations.

The influence of GB thickness and TiC grain size on the TiC layer growth as a function of temperature and time are simulated using the fixed multiplier and a Cu–Sn–Ti–Zr filler alloy of 50 μm thickness as shown in Fig. 6 together with experimental data [14] for a comparison. It is found that simulation fits best for a

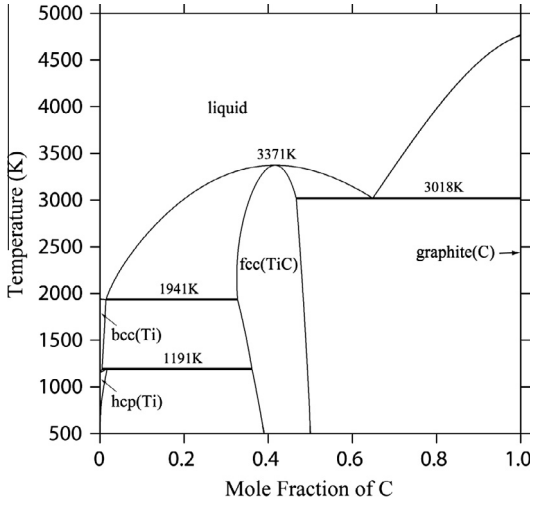

Fig. 2. Calculated phase diagram of the Ti–C binary system according to Frisk [28].

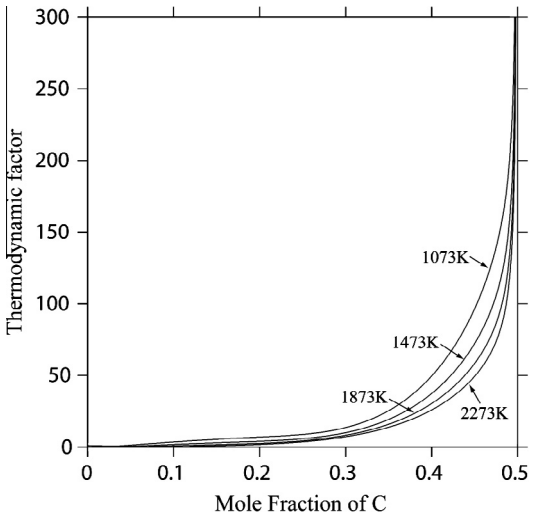

Fig. 3. Calculated thermodynamic factor of the fcc TiC phase in the Ti–C binary system at the different temperatures using the data from Frisk [28].

GB thickness of 1 nm and a grain size of 50 nm, which is in agreement with the experimental observations of TiC grain formed between Cu–Sn–Ti filler and diamond [11,12]. Therefore, the GB thickness and the grain size are preliminarily determined to be 1 nm and 50 nm, which will be used in the following simulations of TiC growth.

Table 1
Mobility parameters of the face-centered cubic TiC alloys.

Mobility	Parameters (J/mol-atoms)	Reference
Mobility of C	$\Delta G_C^{Ti:C} = -406517 + RTln(6.125 \times 10^{-3})$	This work
	$\Delta G_C^{Ti:Va} = -147723 + RTln(2.343 \times 10^{-5})$	[54]
	$\Delta^0 G_C^{Ti:C,Va} = -44627 - 58.258 \times T$	This work
Mobility of Ti	$\Delta G_{Ti}^{Ti:C} = -749696 + RTln(4.7587)$	This work
	$\Delta G_{Ti}^{Ti:Va} = -256900 + RTln(8.600 \times 10^{-5})$	[52]

To validate these values, the growth kinetics of TiC for various Cu–Sn–Ti fillers of 50 μm thickness are simulated and represented in Fig. 7 together with the systematic experimental data [14]. The simulations are in good agreement with the experiments, implying that the values for the multiplier, GB thickness and grain size are reasonable. The growth kinetics of TiC with a typical Ag–Cu–Ti braze alloy of a thickness of 50 μm are also simulated in Fig. 8. The relevant experimental data are often not given or mostly inaccurate [59] except the one for an Ag–Cu–Ti-In alloy [60]. The

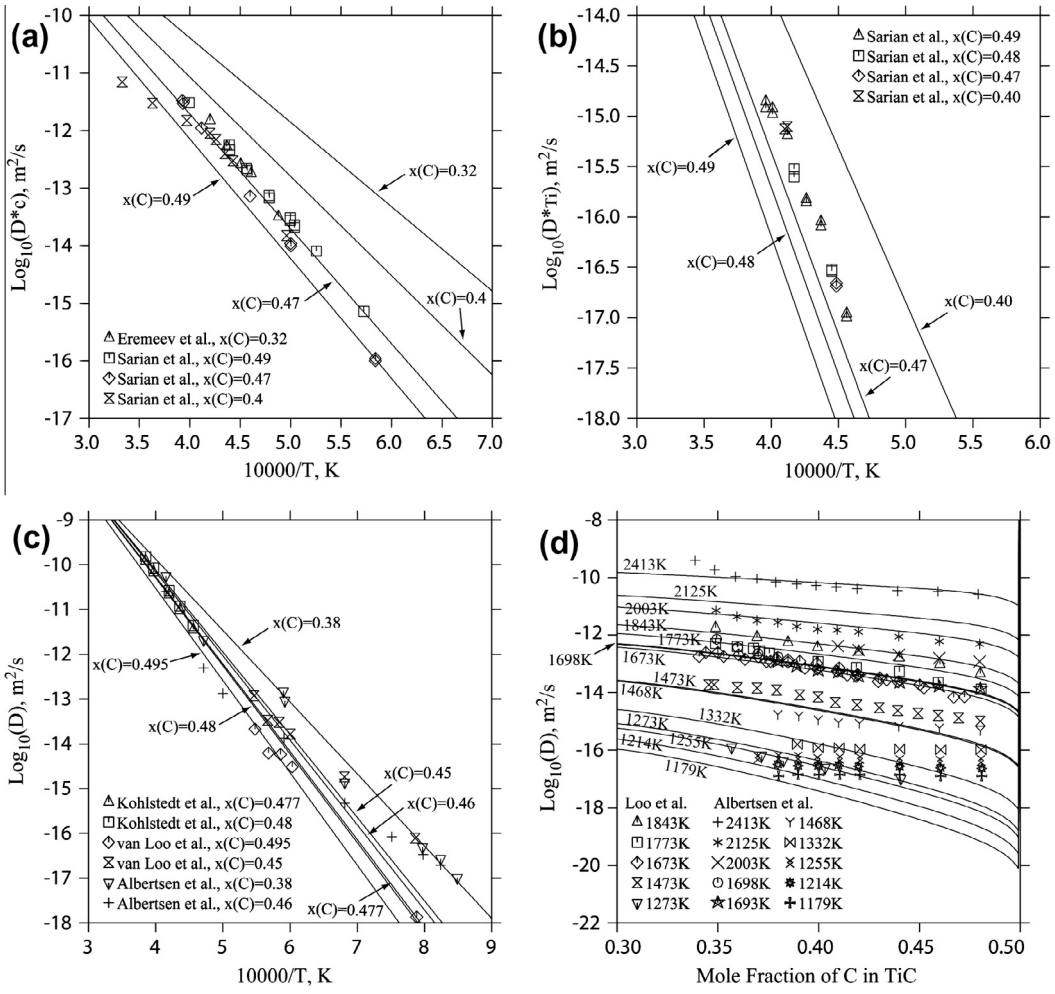

Fig. 4. Calculated temperature dependence of (a) C self-diffusion coefficients in various TiC with experimental data [39–41], (b) Ti self-diffusion coefficients in various TiC with experimental data [42], (c) inter-diffusion coefficients in various TiC with experimental data [48–51], and (d) calculated concentration dependence of inter-diffusion coefficients in the fcc TiC at different temperatures with experimental data [49–51].

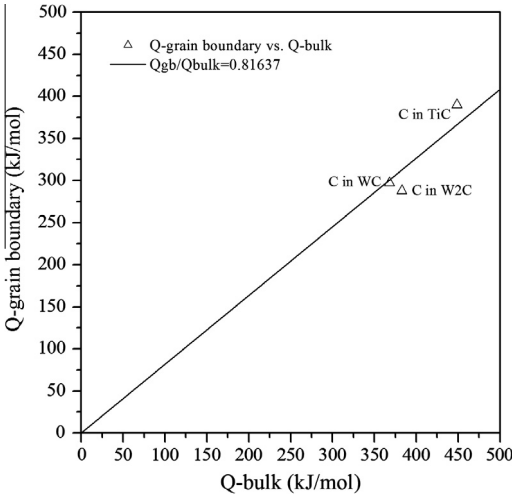

Fig. 5. Determination of average multiplier Q_{gb}/Q_{bulk} by linear fitting the diffusion activation energies of grain boundary and bulk using the available and reliable self-diffusion data [40,55–58] of C in metallic carbides.

elemental analysis reveals insolubility of In in the TiC layer [60], and the thickness is thus reasonably predicted by the present simplified simulation.

4.2. Effect of brazing temperature

Both calculated and measured thicknesses of the TiC layer are plotted against the brazing temperature (cf. Fig. 9). The measured thicknesses are the overall thicknesses of the TiC layer consisting of a cuboidal and a columnar layer taken from the measurements reported in [14]. As seen in Fig. 9, all the calculated data are located in the range of the experimental errors. The brazing temperature appears to have a strong effect on the TiC layer thickness, which shows a pronounced increase with the brazing temperature at a constant dwell time.

4.3. Effect of filler alloy composition

Considering Ti is the important active element of filler in brazing of diamond, the effect of Ti concentration in typical Cu–15 wt.%Sn–*x*Ti (*x* = 2, 5, 10, 15, 20 wt.%) filler alloys of 50 μm thickness on TiC growth at a brazing temperature 930 °C are simulated (Fig. 10). The growth curves of TiC are parabolic, implying

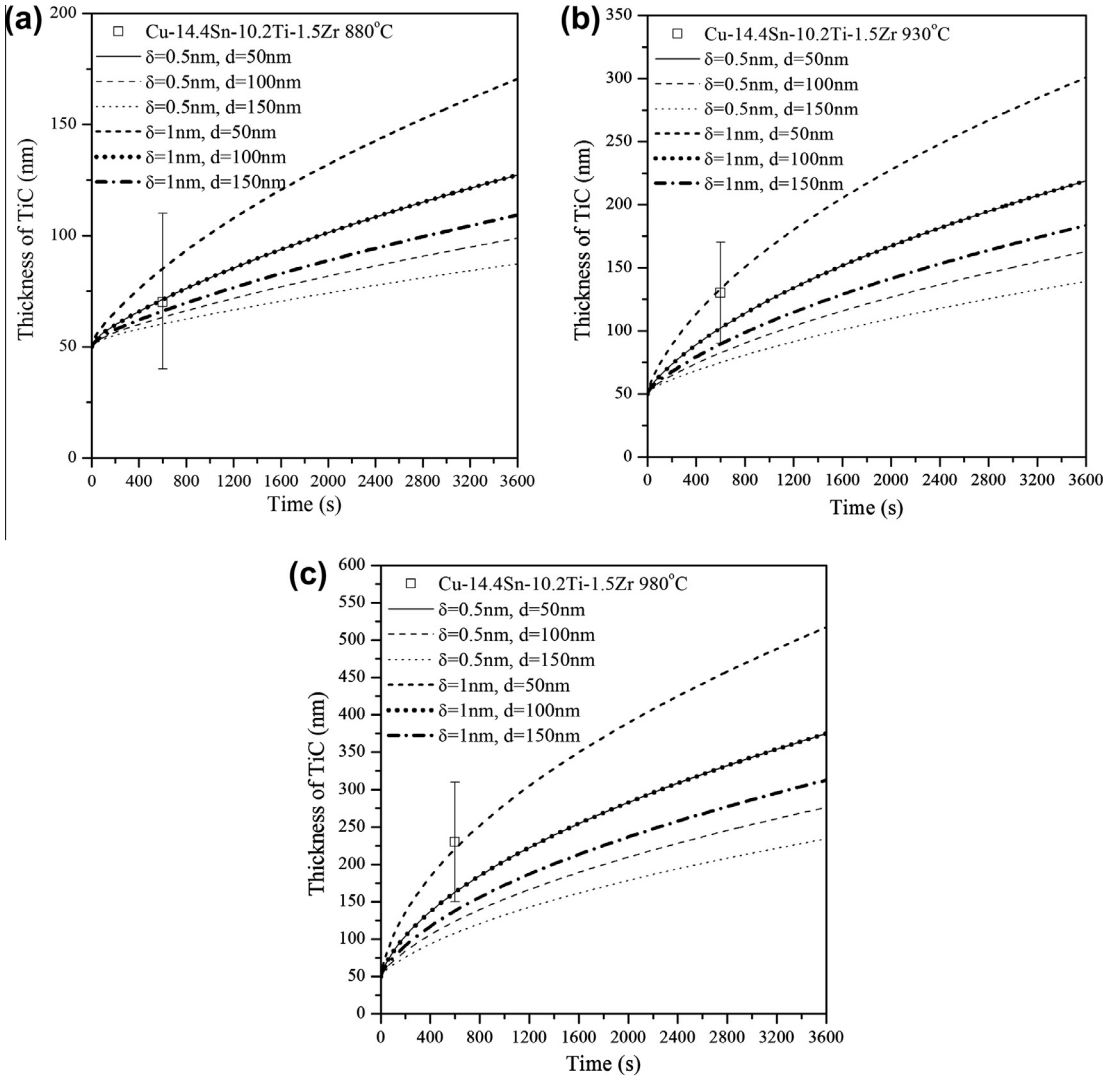

Fig. 6. Simulated TiC growth during brazing of diamond with Cu–14.4Sn–10.2Ti–1.5Zr (wt.%) filler alloy using a fixed multiplier of Q_{gb}/Q_{bulk} = 0.81637, brazing layer thickness of 50 μm, and various GB thicknesses and grain sizes, together with the experimental data [14] (a) at 880 °C (b) at 930 °C and (c) at 980 °C.

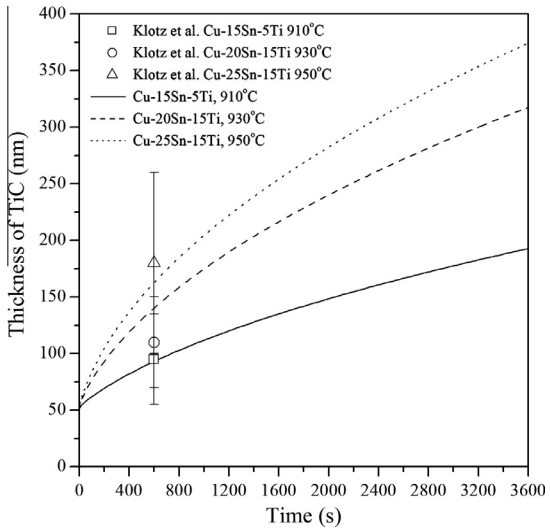

Fig. 7. Simulated TiC growth in brazing diamond with Cu–Sn–Ti fillers at different temperatures with the experimental data [14] using multiplier of 0.81637, GB thickness of 1 nm, TiC grain size of 50 nm, and brazing layer thickness of 50 μm.

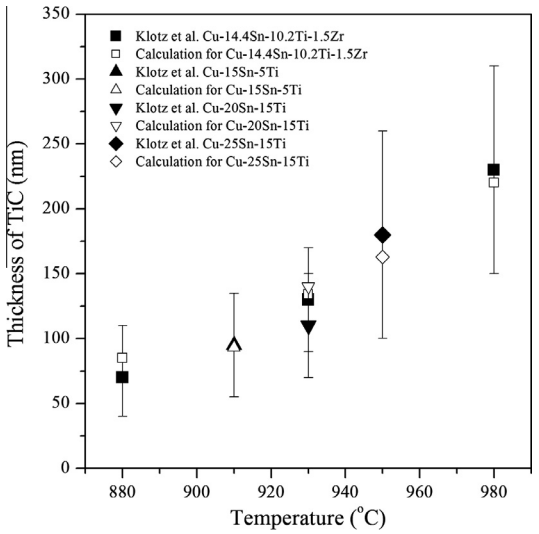

Fig. 9. Calculated and measured TiC layer thickness as a function of brazing temperature and alloy composition (Brazing time is 10 min and the experimental data are taken from [14]).

the diffusion-controlled growth. The thickness of TiC is found to increase with increasing Ti concentration at the same reaction time. For example, after brazing reaction at 930 °C for 1 h, the layer thickness of TiC reaches 195, 241, 293, 337, 380 nm for 2, 5, 10, 15, 20 wt.%Ti, respectively. The higher Ti concentration can supply more Ti to form the TiC layer with C, and consequently result in the faster growth of TiC.

4.4. Effect of braze layer thickness

Aside from the filler alloy composition, the thickness of the braze layer is another important brazing process factor to affect the TiC growth kinetics. The effect of brazing layer thickness of typical Cu–15Sn–10Ti (wt.%) filler on the TiC growth at 930 °C are simulated in Fig. 11a. The Ti concentrations in the fillers close to the TiC/filler interfaces are shown in Fig. 11b. All the TiC growth curves are found to increase with prolonged reaction time for different brazing layer thicknesses of 1, 10, 50, and 100 μm. The Ti contents in the fillers are continuously consumed accompanied with the TiC growth. The TiC growth rate approaches zero for a brazing layer of 1 μm and a reaction time of 1 h. This implies almost no supply of Ti to form additional TiC, and can be explained by the full consumption of Ti in the filler. The braze layer thickness plays a notable role in facilitating the growth of TiC (Fig. 11a) because the thicker filler can supply more Ti to reaction with C. The role is increasingly insignificant with increasing thickness, and become negligible when the thickness reaches 50 μm (Fig. 11b).

4.5. Segregation of Cu at diamond-TiC interface

Khalid et al. [13] observed a thin Cu-rich layer formed at the diamond surface accompanied by the formation of a cuboidal TiC layer at the interface between diamond and a Cu–Sn–Ti–Zr brazing alloy. The majority of the cuboidal TiC particles were found to grow along diamond (100) planes, while no orientation relationship of the Cu-rich particles with the diamond was found. Klotz et al.

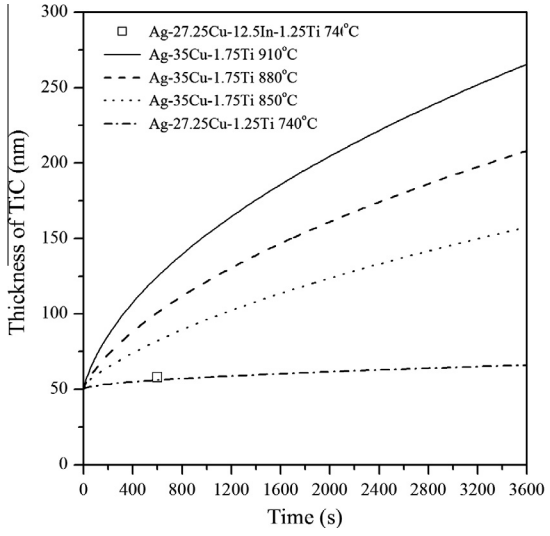

Fig. 8. Simulated TiC growth in brazing diamond with Ag–Cu–Ti filler with the experimental data [59] using multiplier of 0.81637, GB thickness of 1 nm, TiC grain size of 50 nm, and brazing layer thickness of 50 μm.

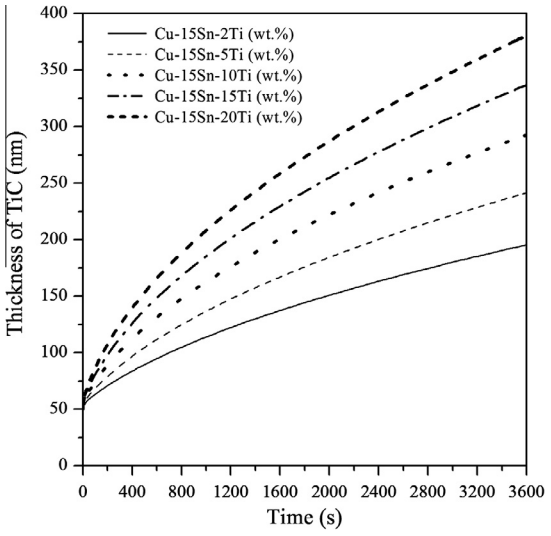

Fig. 10. Simulated influence of Ti amount on TiC growth at 930 °C for Cu–15wt.%Sn–*x*Ti (*x* = 2, 5, 10, 15, 20 wt.%) filler alloy of 50 μm initial thickness.

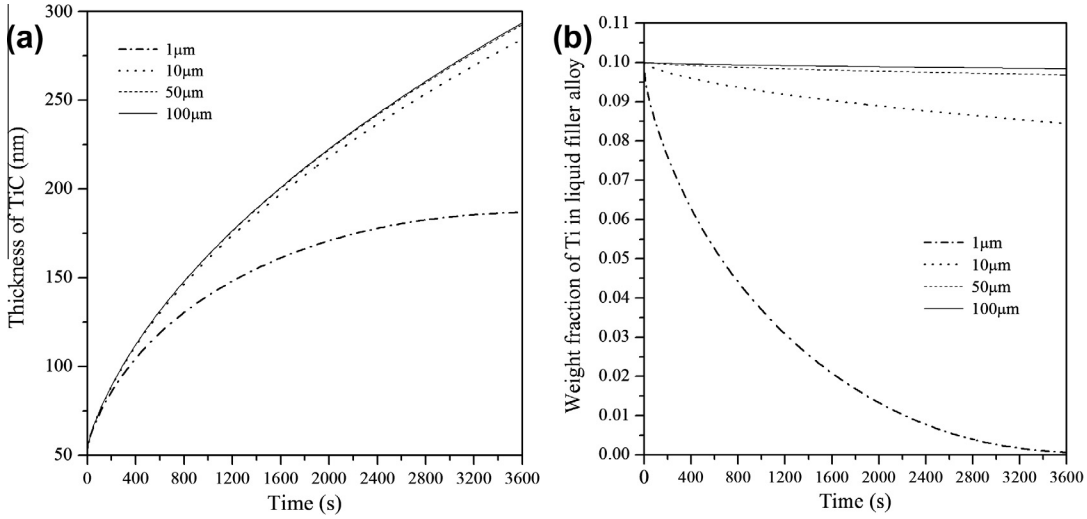

Fig. 11. Simulated influence of braze layer thickness (1, 10, 50, 100 μm) on (a) TiC growth and (b) filler composition in brazing diamond with Cu–15Sn–10Ti (wt.%) filler alloy at 930 °C.

[14] also observed a very thin Cu-rich layer formed directly on diamond (1 1 1) planes between diamond and TiC during brazing with different Cu–Sn–Ti alloys. The cuboidal TiC particles were observed to grow onto the diamond with a preferred orientation relationship. Excessive Cu of the brazing alloy was obviously expelled and accumulated as nano-sized particles at the diamond-TiC interface. The Cu-rich particles showed an epitaxy with the TiC crystallites and non-epitaxy with diamond. The formation of Cu-rich particles was also observed in the Ag–Cu eutectic matrix phase during brazing of diamond with Ag–Cu–In–Ti alloy [60].

The enrichment and precipitation of Cu might affect the stress distribution in diamond and TiC as well as the bond strength since it results in a discontinuous TiC layer. As a preliminary step towards a better understanding of the segregation of Cu, diffusion simulations were carried out. Therefore, additional mobility parameters of Ag, C, Cu, Sn and Ti were required. The mobility parameters of Ag in hypothetical fcc AgC, CuC and SnC are approximated to those of Ag in fcc Ag, Cu and Sn, respectively [61]. The mobility of Ag in TiC is assumed to be that in fcc Ti, which can be obtained by an empirical approach [62] and the related data [52]. The mobilities of C in fcc AgC, CuC and SnC are assumed to be the same as those in fcc NiC [25]. The mobilities of C in fcc Ag, Cu and Sn are all taken from the parameters in fcc Ni [25]. As for the mobility of Cu, similar assumptions are made and all parameters are taken from the literature [52,61,63,64]. Most of the parameters of Sn are available [61,64] and the mobility of Sn in fcc Ti or TiC is evaluated from that of Cu in fcc Ti [52]. All parameters for Ti are taken from the data in [65,66] with the assumption that the mobility of Ti in fcc Sn or SnC is regarded as that of Ti in fcc Cu. All the interaction parameters [61] of Ag, Cu, Sn are available and then adopted.

The simulated concentration profiles through brazing sectional structures, respectively for Cu–15Sn–10Ti (wt.%) and Ag–35Cu–1.75Ti (wt.%), are shown in Fig. 12. At the beginning, no extra product appears in addition to TiC. With the movement of the TiC-filler interface, i.e. thickening of the TiC layer, Cu enriches and precipitates as a Cu-rich layer at the diamond-TiC interface in a rather short time. Considering the similar crystal structure of Ag and Cu to TiC, and the smaller atomic radius of Cu, the diffusion mobility of Cu in TiC is higher than the ones of Ag and Sn. Thus, Cu rather than other elements will dominate the diffusion through TiC and enrich preferentially at the interface.

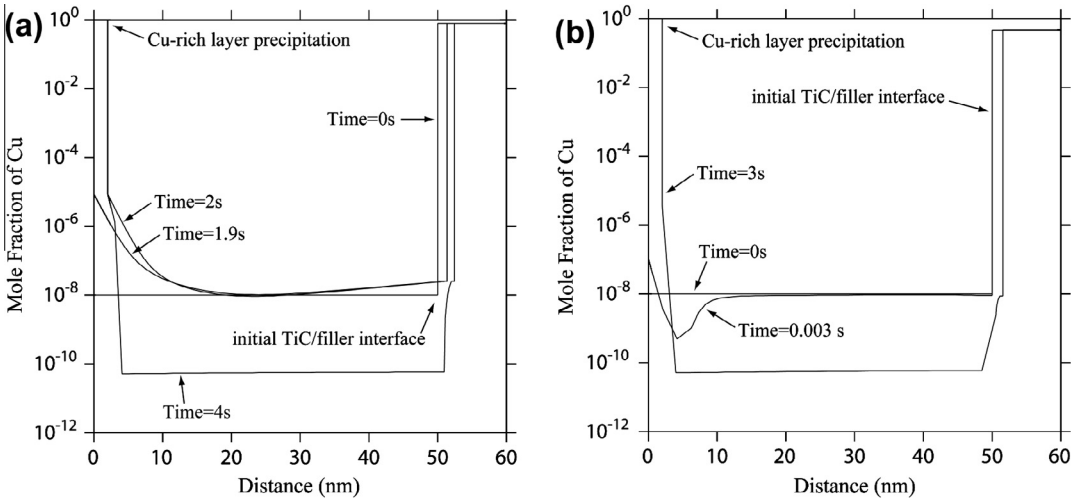

Fig. 12. Simulated concentration–distance profile perpendicular to the TiC/filler alloy interface during brazing with (a) Cu–15Sn–10Ti (wt.%) at 980 °C; and (b) Ag–35Cu–1.75Ti (wt.%) at 910 °C.

From a thermodynamic point of view, the enrichment and precipitation of Cu probably enables a more stable interface system. Additionally, interfacial stresses and interface energies, caused by the newly formed interfaces diamond–Cu and Cu–TiC, should be considered as the governing factors to determine the morphology of the accumulative Cu. According to the work by Yamazaki and Suzumura [67], the lattice constant of Cu is closer to that of diamond than TiC, so the lattice mismatch between diamond and Cu for the (100)//(100), (110)//(110) or (111)//(111) interfaces is always significantly smaller than that between diamond or Cu and TiC. It is hence believed that the stress relaxation and the thermodynamic stability should be at least a partial reason for the Cu segregation.

5. Conclusions

The growth of TiC reaction layer with Cu–Sn–Ti or Ag–Cu–Ti based filler alloy was investigated by kinetic simulations. The atomic mobility database of TiC was obtained by evaluating available diffusion data. The activation energy multiplier, GB thickness, and grain size of TiC were assessed and validated to be 0.81637, 1 nm, and 50 nm, respectively. Influences of brazing temperature, filler alloy composition, and braze layer thickness on the growth kinetics of TiC were successfully simulated. The simulated results indicate TiC grows almost linearly with increased brazing temperature, faster with more Ti amount in the filler, and more rapidly with the thicker braze layer. The segregation of Cu at the diamond-TiC interface was simulated and interpreted. The enrichment and precipitation of Cu will result in more stable interface. The smaller misfit between diamond and Cu can lead to the lower stress.

Acknowledgements

The present work was funded by the Sino Swiss Science and Technology Cooperation (SSSTC) within the Project no. IZLCZ2 138905.

Appendix A. Supplementary material

Supplementary data associated with this article can be found, in the online version, at http://dx.doi.org/10.1016/j.commatsci.2013.05.025.

References

[1] K. Suganuma, Y. Miyamoto, M. Koizumi, Ann. Rev. Mater. Sci. 18 (1988) 47–73.
[2] J.M. Howe, Int. Mater. Rev. 38 (1993) 233–256.
[3] J.M. Howe, Int. Mater. Rev. 38 (1993) 257–271.
[4] S.B. Sinnott, E.C. Dickey, Mater. Sci. Eng. R 43 (2003) 1–59.
[5] S.S. Babu, Int. Mater. Rev. 54 (2009) 333–367.
[6] N.Y. Taranets, Y.V. Naidich, J. Adhesion Sci. Tech. 23 (2009) 2121–2132.
[7] J.H. Kim, Y.C. Yoo, Mater. Sci. Tech. 14 (1998) 352–356.
[8] Y.N. Liang, M.I. Osendi, P. Miranzo, J. Eur. Ceram. Soc. 23 (2003) 547–553.
[9] H.P. Xoing, B. Chen, Y.S. Kang, W. Mao, A. Kawasaki, H. Okamura, R. Watanabe, Scripta Mater. 56 (2007) 173–176.
[10] H.P. Xiong, W. Dong, B. Chen, Y.S. Kang, A. Kawasaki, H. Okamura, R. Watanabe, Mater. Sci. Eng. A 474 (2008) 376–381.
[11] W.C. Li, C. Liang, S.T. Lin, Diam. Relat. Mater. 11 (2002) 1366–1373.
[12] W.C. Li, C. Liang, S.T. Lin, Metall. Mater. Trans. A 33 (2002) 2163–2172.
[13] F.A. Khalid, U.E. Klotz, H.-R. Elsener, B. Zigerlig, P. Gasser, Scripta Mater. 50 (2004) 1139–1143.
[14] U.E. Klotz, C.L. Liu, F.A. Khalid, H.-R. Elsener, Mater. Sci. Eng. A 495 (2008) 265–270.
[15] M. Akbari, S. Buhl, C. Leinenbach, R. Spolenak, K. Wegener, Mech. Mater. 52 (2012) 69–77.
[16] S. Buhl, C. Leinenbach, R. Spolenak, K. Wegener, Int. J. Refract. Met. Hard Mater. 30 (2012) 16–24.
[17] J.-O. Andersson, L. Höglund, B. Jönsson, J. Ågren, in: G.R. Purdy (Ed.), Fundamentals and Applications of Ternary Diffusion, Pergamon Press, New York, 1990, pp. 153–163.
[18] J.-O. Andersson, J. Ågren, J. Appl. Phys. 72 (1992) 1350–1355.
[19] A. Borgenstam, A. Engström, L. Höglund, J. Ågren, J. Phase Equilib. 21 (2000) 269–280.
[20] A. Bjärbo, Scand. J. Metall. 32 (2003) 94–99.
[21] J. Ågren, Scand. J. Metall. 19 (1990) 2–8.
[22] O. Prat, J. Garcia, D. Rojas, C. Carrasco, A.R. Kaysser-Pyzalla, Mater. Sci. Eng. A 527 (2010) 5976–5983.
[23] J. Ågren, Iron Steel Inst. Jpn. Int. 32 (1992) 291–296.
[24] B. Jönsson, Z. Metallkd. 85 (1994) 498–501.
[25] B. Jönsson, Z. Metallkd. 85 (1994) 502–509.
[26] B. Jönsson, Z. Metallkd. 83 (1992) 349–355.
[27] O. Redlich, A. Kister, Ind. Eng. Chem. 40 (1948) 345–348.
[28] K. Frisk, CALPHAD 27 (2003) 367–373.
[29] I.I. Gorbachev, V.V. Popov, Phys. Met. Metallogr. 108 (2009) 484–495.
[30] X.C. He, H. Wang, H.S. Liu, Z.P. Jin, CALPHAD 30 (2006) 367–374.
[31] O. Dezellus, R. Arroyave, S.G. Fries, Int. J. Mat. Res. 102 (2011) 286–297.
[32] K.-W. Moon, W.J. Boettinger, U.R. Kattner, F.S. Biancaniello, C.A. Handwerker, J. Electron. Mater. 29 (2000) 1122–1136.
[33] A. Fernández Guillermet, J. Alloys Compds. 217 (1995) 69–89.
[34] J. Wang, C.L. Liu, C. Leinenbach, U.E. Klotz, P.J. Uggowitzer, J.F. Löffler, CALPHAD 35 (2011) 82–94.
[35] R. Jerlerud Pérez, C. Toffolon-Masclet, J.-M. Joubert, B. Sundman, CALPHAD 32 (2008) 593–601.
[36] R. Arroyave, T.W. Eagar, L. Kaufman, J. Alloys Compds. 351 (2003) 158–170.
[37] J.S. Kirkarldy, D.J. Young, Inst. Met. (1987).
[38] B.-J. Lee, N.M. Hwang, H.M. Lee, Acta Mater. 45 (1997) 1867–1874.
[39] V.S. Eremeev, A.S. Panov, Porosh. Met. Akad. Nauk. Ukr. SSR 7 (1967) 65–69.
[40] S. Sarian, J. Appl. Phys. 39 (1968) 3305–3310.
[41] S. Sarian, J. Appl. Phys. 39 (1968) 5036–5041.
[42] S. Sarian, J. Appl. Phys. 40 (1969) 3515–3520.
[43] L.M. Adelsberg, L.H. Cadoff, Trans. AIME 239 (1967) 933–935.
[44] C.A. Vansant, W.C. Phelps Jr., Trans. ASM 59 (1966) 105–112.
[45] A.V. Shcherbedinskaya, A.N. Minkevich, Tsvetn. Met. 8 (1965) 123–125.
[46] K. Kōyama, Y. Hashimoto, S. Ōmori, Trans. Jpn. Inst. Metals 16 (1975) 211–217.
[47] C.J. Quinn, D.L. Kohlstedt, J. Am. Chem. Soc. 67 (1984) 305–310.
[48] D.L. Kohlstedt, W.S. Williams, J.B. Woodhouse, J. Appl. Phys. 41 (1970) 4476–4484.
[49] F.J.J. van Loo, W. Wakelkamp, G.F. Bastin, R. Metselaar, Solid State Ionics 32 (33) (1989) 824–832.
[50] F.J.J. van Loo, G.F. Bastin, Metall. Trans. A 20 (1989) 403–411.
[51] K. Albertsen, H.-J. Schaller, Ber. Bunsenges. Phys. Chem. 98 (1994) 1224–1230.
[52] N. Matan, H.M.A. Winand, P. Carter, M. Karunaratne, P.D. Bogdanoff, R.C. Reed, Acta Mater. 46 (1998) 4587–4600.
[53] C.E. Campbell, W.J. Boettinger, U.R. Kattner, Acta Mater. 50 (2002) 775–792.
[54] S. Movlanov, A.A. Kuliev, Phys. Solid State 4 (1962) 394–396.
[55] V.M. Sura, D.L. Kohlstedt, J. Mater. Sci. 21 (1986) 2347–2355.
[56] V.M. Sura, D.L. Kohlstedt, J. Mater. Sci. 21 (1986) 2356–2364.
[57] C.P. Bushmer, P.H. Crayton, J. Mater. Sci. 6 (1971) 981–983.
[58] D. Treheux, J. Dubois, G. Fantozzi, Ceram. Int. 7 (1981) 142–148.
[59] A. Palavra, A.J.S. Fernandes, C. Serra, F.M. Costa, L.A. Rocha, R.F. Silva, Diam. Relat. Mater. 10 (2001) 775–780.
[60] U.E. Klotz, F.A. Khalid, H.-R. Elsener, Diam. Relat. Mater. 15 (2006) 1520–1524.
[61] W. Gierlotka, Y.H. Chen, M.A. Haque, M.A. Rahman, J. Electron. Mater. 41 (2012) 3359–3367.
[62] Y. Du, L.J. Zhang, S.L. Cui, D.D. Zhao, D.D. Liu, W.B. Zhang, W.H. Sun, W.Q. Jie, Sci. China Tech. Sci. 55 (2012) 1–23.
[63] G. Ghosh, Acta Mater. 49 (2001) 2609–2624.
[64] J. Wang, C. Leinenbach, H.S. Liu, L.B. Liu, M. Roth, Z.P. Jin, CALPHAD 33 (2009) 704–710.
[65] H. Mehrer, D. Weiler, Z. Metallkd. 75 (1984) 203–205.
[66] J. Wang, C. Leinenbach, L.B. Liu, H.S. Liu, Z.P. Jin, J. Phase Equilib, Diff. 32 (2011) 30–38.
[67] T. Yamazaki, A. Suzumura, J. Mater. Sci. 35 (2000) 6155–6160.